Environmental Science Processes & Impacts

PAPER

View Article Online
View Journal | View Issue

Cite this: *Environ. Sci.: Processes Impacts*, 2018, **20**, 1524

Development of a hydrophilic interaction liquid chromatography (HILIC) method for the chemical characterization of water-soluble isoprene epoxydiol (IEPOX)-derived secondary organic aerosol†

Tianqu Cui,‡[a] Zhexi Zeng,‡[a] Erickson O. dos Santos,[b] Zhenfa Zhang,[a] Yuzhi Chen,[a] Yue Zhang,[ac] Caitlin A. Rose,[a] Sri H. Budisulistiorini,§[a] Leonard B. Collins,[a] Wanda M. Bodnar,[a] Rodrigo A. F. de Souza,[d] Scot T. Martin,[ef] Cristine M. D. Machado,[b] Barbara J. Turpin,[a] Avram Gold,[a] Andrew P. Ault[gh] and Jason D. Surratt*[a]

Acid-catalyzed multiphase chemistry of isoprene epoxydiols (IEPOX) on sulfate aerosol produces substantial amounts of water-soluble secondary organic aerosol (SOA) constituents, including 2-methyltetrols, methyltetrol sulfates, and oligomers thereof in atmospheric fine particulate matter ($PM_{2.5}$). These constituents have commonly been measured by gas chromatography interfaced to electron ionization mass spectrometry (GC/EI-MS) with prior derivatization or by reverse-phase liquid chromatography interfaced to electrospray ionization high-resolution mass spectrometry (RPLC/ESI-HR-MS). However, both techniques have limitations in explicitly resolving and quantifying polar SOA constituents due either to thermal degradation or poor separation. With authentic 2-methyltetrol and methyltetrol sulfate standards synthesized in-house, we developed a hydrophilic interaction liquid chromatography (HILIC)/ESI-HR-quadrupole time-of-flight mass spectrometry (QTOFMS) protocol that can chromatographically resolve and accurately measure the major IEPOX-derived SOA constituents in both laboratory-generated SOA and atmospheric $PM_{2.5}$. 2-Methyltetrols were simultaneously resolved along with 4–6 diastereomers of methyltetrol sulfate, allowing efficient quantification of both major classes of SOA constituents by a single non-thermal analytical method. The sum of 2-methyltetrols and methyltetrol sulfates accounted for approximately 92%, 62%, and 21% of the laboratory-generated β-IEPOX aerosol mass, laboratory-generated δ-IEPOX aerosol mass, and organic aerosol mass in the southeastern U.S., respectively, where the mass concentration of methyltetrol sulfates was 171–271% the mass concentration of methyltetrol. Mass concentrations of methyltetrol sulfates were 0.39 and 2.33 μg m^{-3} in a $PM_{2.5}$ sample collected from central Amazonia and the southeastern U.S., respectively. The improved resolution clearly reveals isomeric patterns specific to methyltetrol sulfates from acid-catalyzed multiphase chemistry of β- and δ-IEPOX. We also demonstrate that conventional GC/EI-MS analyses overestimate 2-methyltetrols by up to 188%, resulting (in part) from the thermal degradation of methyltetrol sulfates. Lastly, C_5-alkene triols and 3-methyltetrahydrofuran-3,4-diols are found to be largely GC/EI-MS artifacts formed from thermal degradation of 2-methyltetrol sulfates and 3-methyletrol sulfates, respectively, and are not detected with HILIC/ESI-HR-QTOFMS.

Received 10th July 2018
Accepted 15th September 2018

DOI: 10.1039/c8em00308d

rsc.li/espi

[a]*Department of Environmental Sciences and Engineering, Gillings School of Global Public Health, The University of North Carolina at Chapel Hill, Chapel Hill, North Carolina, USA. E-mail: surratt@unc.edu; Fax: +1-919-966-7911; Tel: +1-919-966-0470*

[b]*Department of Chemistry, Federal University of Amazonas, Manaus, Amazonas, Brazil*

[c]*Aerodyne Research Inc., Billerica, Massachusetts, USA*

[d]*Superior School of Technology, University of the State of Amazonas, Manaus, Amazonas, Brazil*

[e]*School of Engineering and Applied Sciences, Harvard University, Cambridge, Massachusetts, USA*

[f]*Department of Earth and Planetary Sciences, Harvard University, Cambridge, Massachusetts, USA*

[g]*Department of Environmental Health Sciences, University of Michigan, Ann Arbor, Michigan, USA*

[h]*Department of Chemistry, University of Michigan, Ann Arbor, Michigan, USA*

† Electronic supplementary information (ESI) available. See DOI: 10.1039/c8em00308d

‡ These authors contributed equally to the work presented here.

§ Current address: Earth Observatory of Singapore, Nanyang Technological University, Singapore.

Environmental significance

$PM_{2.5}$ adversely affects air quality and human health. Isoprene is the most abundant non-methane volatile organic compound primarily emitted from biogenic sources to Earth's atmosphere. Atmospheric oxidation of isoprene yields large quantities of gaseous IEPOX by hydroxyl radicals under low-nitric oxide conditions. IEPOX subsequently undergoes acid-catalyzed multiphase chemistry with natural or anthropogenic sulfate aerosol, producing substantial amounts of water-soluble IEPOX-derived SOA in $PM_{2.5}$. The HILIC/ESI-HR-QTOFMS method presented here overcomes limitations of commonly utilized analytical techniques, making it possible to identify and quantify water-soluble SOA constituents by a single analytical method. Atmospheric chemistry model predictions of the water-soluble IEPOX-derived SOA constituents (*e.g.*, 2-methyltetrols and methyltetrol sulfates) in $PM_{2.5}$ can now be assessed with greater accuracy and confidence.

1. Introduction

Atmospheric fine particulate matter ($PM_{2.5}$, aerosol particles with aerodynamic diameters $\leq$ 2.5 μm) adversely affects air quality. High concentrations of $PM_{2.5}$ can lead to degradation of outdoor visibility[1] and adversely affect human health through cardiovascular and respiratory diseases.[2] Moreover, atmospheric $PM_{2.5}$ plays a critical role in climate change through both direct and indirect mechanisms.[3] Organic aerosol (OA) constituents are recognized to contribute a substantial fraction of $PM_{2.5}$ mass from urban to remote regions around the world.[4] OA is further characterized into primary organic aerosol (POA) and secondary organic aerosol (SOA). POA is directly emitted in the particle phase from sources, such as sea spray, wildfires, automobiles and cooking, while SOA is formed from the atmospheric oxidation of volatile organic compounds (VOCs) emitted by both anthropogenic and natural sources. Specifically, low volatile oxidation products from VOCs either nucleate or condense onto existing particles and undergo multiphase chemistry to form SOA, which is estimated to contribute 70–90% of OA mass found within $PM_{2.5}$.[5]

Isoprene is the most abundant non-methane hydrocarbon emitted into Earth's atmosphere and is derived largely from deciduous trees.[6] The atmospheric oxidation of isoprene plays an important role in both tropospheric ozone (O_3) and SOA formation in forested regions affected by anthropogenic activities.[7–14] The hydroxyl radical (OH)-initiated oxidation of isoprene during the daytime under low-nitric oxide (NO) conditions produces substantial amounts of isoprene epoxydiols (IEPOX) (~50% yield).[15,16] The acid-catalyzed multiphase chemistry (reactive uptake) of IEPOX onto anthropogenic sulfate particles have been shown to produce SOA constituents including 2-methyltetrols,[8,9,17,18] C_5-alkene triols,[8,9,17,18] 3-methyltetrahydrofuran-3,4-diols (3-MeTHF-3,4-diols),[9] organosulfates,[9,18–20] and oligomers.[9,18,21] Studies have also pointed out that the mixed effects of sulfate (*e.g.*, aerosol acidity, nucleophile, surface area, and salting-in) play a critical role in forming atmospheric IEPOX-derived SOA.[10,19,22–24]

Protocols for chemical characterization of IEPOX-derived SOA C_5 tracers, including the 2-methyltetrols, C_5-alkene triols, and 3-MeTHF-3,4-diols, have generally employed gas chromatography interfaced to electron ionization mass spectrometry (GC/EI-MS) with prior trimethylsilylation.[8,9,17–19,25] These tracer species have been widely used to investigate SOA formation mechanisms, derive kinetic parameters, and evaluate model performance of IEPOX-derived SOA.[9,17,26,27] However, volatility and composition analysis by a Filter Inlet for Gases and Aerosol coupled to a Chemical Ionization Mass Spectrometer (FIGAERO-CIMS) equipped with iodide reagent ion chemistry demonstrated that IEPOX-derived SOA has lower volatility than predicted from the concentrations of commonly reported IEPOX SOA C_5 tracers, in particular the 2-methyltetrols, C_5-alkene triols and 3-MeTHF-3,4-diols, and therefore thermal decomposition of accretion products (oligomers) or other low volatile organics such as organosulfates may contribute significantly to tracers.[28] A second set of studies using FIGAERO-CIMS or semi-volatile thermal desorption aerosol gas chromatogram (SV-TAG) instrumentation with online derivatization reached similar conclusions on the impact of thermal decomposition.[29–32] Different protocols, based on ultra-performance liquid chromatography interfaced to high-resolution tandem mass spectrometry with electrospray ionization (UPLC/ESI-HR-MS^n), have been used to characterize organosulfates and oligomers. However, separation of polar, water-soluble components is conventionally attempted with reverse-phase liquid chromatography (RPLC) columns.[8,9,19,33] RPLC columns do not resolve such compounds well because of either extremely short retention times (RTs), poor peak shapes, or ion suppression effects due to co-eluting inorganic aerosol constituents, leading to potential complications in identifying and quantifying target compounds. The IEPOX-derived polyols are hydrophilic compounds owing to their hydroxyl functional groups, and the organosulfates are ionic polar compounds.[28,33] Hence, an alternative approach for the IEPOX-derived SOA characterization that could accomplish simultaneous analysis of polar and water-soluble components while avoiding the drawbacks associated with current analytical methods would be highly desirable.

Hydrophilic interaction liquid chromatography (HILIC) is as an alternative LC method to RPLC to separate hydrophilic (*i.e.*, water-soluble) compounds, including peptides and nucleic acids[34] and has recently been reported to separate water-soluble organosulfates with excellent resolution.[35–37] The HILIC solid phase can be silica gel with a decreased surface concentration of silanol groups, or silica chemically bonded to polar groups, such as amino, amide, cyano, carbamate, diol, polyol, or zwitterionic sulfobetaine groups.[38] A HILIC column separates analytes by forming a water-rich layer, which is partially immobilized around the hydrophilic ligands on the stationary phase. Analytes can undergo partitioning between the bulk organic eluents and the water-rich layer to separate based on different levels of retention.[39] Although retention order on

HILIC columns is similar to that on normal phase liquid chromatography (NPLC) columns, HILIC utilizes more polar mobile phases (*e.g.*, acetonitrile (ACN) and Milli-Q water) than the NPLC so that the HILIC method is compatible for interfacing with ESI-MS sources.[40] ESI is a soft ionization detection method not involving sample heating or derivatization and is appropriate for detection of polar C_5 tracers, and oligomers as well as water-soluble organosulfates. Based on the demonstrated success of HILIC in the chemical characterization of organosulfates from synthesized standards and field samples,[35–37] we undertook development of a HILIC/ESI-HR-quadrupole time-of-flight mass spectrometry (HILIC/ESI-HR-QTOFMS) method for the simultaneous separation, characterization, and quantitation of water-soluble IEPOX-derived SOA constituents from laboratory-generated β-IEPOX and δ-IEPOX SOA as well as $PM_{2.5}$ collected from the southeastern U.S. at Look Rock, Tennessee (TN), during Southern Oxidant and Aerosol Study (SOAS) in 2013 and central Amazonia at Manaus, Brazil in 2016. The HILIC/ESI-HR-QTOFMS protocol developed here can resolve IEPOX-derived 2-methyltetrols, methyltetrol sulfates and oligomers thereof, allowing unambiguous identification and quantification. Current atmospheric models explicitly simulate SOA from the acid-catalyzed multiphase chemistry of IEPOX (*i.e.*, the formation of 2-methyltetrols and methyltetrol sulfates),[27,41–43] and the accurate quantification of the 2-methyltetrols and the derived organosulfates will increase confidence in evaluation of model predictions, which will in turn lead to improved modeling. Improvement in quantification of organosulfates will additionally provide much needed data for establishing carbon and sulfur mass closure in IEPOX-derived SOA measured or predicted during future lab and field studies.

2. Experiment section

2.1 Synthesized chemicals

2.1.1. *Trans*-β- and δ-IEPOX. Racemic *trans*-β-IEPOX (*trans*-2-methyl-2,3-epoxybutane-1,4-diol) and δ-IEPOX (3-methyl-3,4-epoxy-1,2-butanediol) were synthesized in-house according to published methods.[44,45]

2.1.2. IEPOX-derived SOA standards: 2-methyltetrols, 2-methyltetrol sulfates, and 3-methyltetrol sulfates. Diastereomeric mixtures of racemic 2-methyltetrols (racemic 2-methylerythritol and 2-methylthreitol, molecular weight (MW) = 136 g mol^{-1}) were synthesized by acid hydrolysis of δ-IEPOX according to the procedure described in Bondy *et al.*[44] A diastereomeric mixture of racemic 2-methyltetrol sulfates ((2*R*,3*S*)/(2*S*,3*R*)- and (2*S*,3*S*)/(2*R*,3*R*)-1,3,4-trihydroxy-2-methylbutan-2-yl sulfates, MW = 216 g mol^{-1}; Table 1) was synthesized from 2-methyltetrol. Briefly, the primary and secondary hydroxyl groups of 2-methyltetrol were protected by acetylation with acetic anhydride. The acetylated product was purified by column chromatography on SiO_2, eluted with ethyl acetate and then sulfated by a published procedure.[46] The protecting acetyl groups were then removed by treatment with ammonia to afford the expected diastereomeric 2-methyltetrol sulfates. The purity of the 2-methyltetrol sulfates was determined by proton nuclear magnetic resonance (^{1}H NMR) spectroscopy analysis to be >99% (Fig. S1, in ESI†). The diastereomeric 3-methyltetrol sulfate racemates ((2*R*,3*S*)/(2*S*,3*R*)- and (2*S*,3*S*)/(2*R*,3*R*)-2,3,4-trihydroxy-3-methylbutyl sulfates; MW = 216 g mol^{-1}; Table 1) were prepared from δ-IEPOX by a procedure described in Bondy *et al.*[44] Briefly, to an ice-cold solution of δ-IEPOX in ACN, Bu_4NHSO_4 and a small amount of potassium bisulfate were added and the reaction allowed to warm to room temperature and stirred overnight. The resulting mixture of sulfate esters was purified on a Dowex 50W x4-100 ion exchange column. The final product contained 95.5% 3-methyltetrol sulfates by ^{1}H NMR analysis.

2.2 HILIC/ESI-HR-QTOFMS method

An Agilent 6520 Series Accurate Mass Q-TOFMS instrument interfaced to an Agilent 6500 Series UPLC system, equipped with an ESI source operated in the negative (−) ion mode, was used to chemically characterize IEPOX-derived SOA standards, as well as lab and field samples. Optimum ESI conditions were: 3500 V capillary voltage, 130 V fragmentor voltage, 65 V skimmer voltage, 300 °C gas temperature, 10 L min^{-1} drying gas flow rate, 35 psig nebulizer, 25 psig reference nebulizer. ESI-QTOFMS mass spectra were recorded from mass-to-charge ratio (*m*/*z*) 60 to 1000. HILIC separations were carried out using a Waters ACQUITY UPLC BEH Amide column (2.1 × 100 mm, 1.7 μm particle size, Waters) at 35 °C. The mobile phases consisted of eluent (A) 0.1% ammonium acetate in water, and eluent (B) 0.1% ammonium acetate in a 95 : 5 (v/v) ACN (HPLC Grade, 99.9%, Fisher Scientific)/Milli-Q water. Both eluents were adjusted to a pH of ~9.0 with NH_4OH.[35] The gradient elution program was eluent A, 0% for 4 min, increasing to 15% from 4 to 20 min, constant at 15% between 4 and 24 min, decreasing to 0% from 24 to 25 min, and constant at 0% from 25 to 30 min. The flow rate and sample injection volume were 0.3 mL min^{-1} and 5 μL, respectively. Data were acquired and analyzed by Mass Hunter Version B.06.00 Build 6.0.633.0 software (Agilent Technologies). At the beginning of each analysis period, the mass spectrometer was calibrated using a commercially available ESI-L low-mass concentration tuning mixture (Agilent Technologies) in a 95 : 5 (v/v) ACN/Milli-Q water. Instrument mass axis calibration was conducted in the low-mass range (*m*/*z* 50–1700). Seven masses were used for calibration: *m*/*z* 68.9958, 112.9856, 301.9981, 601.9790, 1033.9881, 1333.9689, and 1633.9498. The adduct of hexakis (1*H*,1*H*,3*H*-tetrafluoropropoxy) phosphazene + acetate (*m*/*z* 980.0164), purine (*m*/*z* 119.0363), and leucine enkephalin (*m*/*z* 554.2620) were continuously infused for real-time mass axis correction. The mass resolution of the ESI-HR-QTOFMS was approximately 8000–12 300 from *m*/*z* 113–1600.

For comparison purposes, RPLC separations (Waters ACQUITY UPLC HSS T3 C_{18} column, 2.1 × 100 mm, 1.8 μm particle size) were also conducted on selected samples that were analyzed by HILIC, where pure methanol (99.9%, Fisher Chemical) was used as the mobile phase (B) and standards and samples were prepared in 50 : 50 Milli-Q water/methanol. The detailed operating procedures for RPLC separations have been

Table 1 Properties of the 2-methyltetrol, 2-methyltetrol sulfate and 3-methyltetrol sulfate standards characterized by HILIC/ESI-HR-Q-TOFMS, including retention times (RTs), linear range (L. range), coefficient of determination (R^2), limit of detection (LOD), limit of quantification (LOQ) of ten replicate injections. Note that structures are for one of two diastereomers for each standard and ions are shown for the methyltetrol sulfates

Standard	Synthesized structural isomer	Structure	$[M-H]^-$	m/z	RT(s) (min)	L. range ($\mu g\ mL^{-1}$)	R^2	LOD ($\mu g\ L^{-1}$)	LOQ ($\mu g\ L^{-1}$)
2-Methyltetrols	2-Methylerythritol and 2-methylthreitol	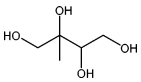	$C_5H_{11}O_4^-$	135.066	4.0	0.01–25	0.9994	7.74	25.8
2-Methyltetrol sulfates	1,3,4-Trihydroxy-2-methylbutan-2-yl sulfate	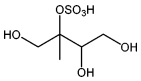	$C_5H_{11}O_7S^-$	215.023	2.1, 2.6, 4.2, 5.2	0.01–10	0.9996	1.72	5.75
3-Methyltetrol sulfates	2,3,4-Trihydroxy-3-methylbutyl sulfate	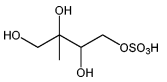	$C_5H_{11}O_7S^-$	215.023	2.1, 2.6, 4.2, 5.2, 8.0, 8.3	0.01–25	1.0000	3.83	12.8

described elsewhere.[47] In addition, GC/EI-MS analysis with prior derivatization was performed following the procedures described previously.[9,18] In brief, a diluted aliquot of each filter extract was dried and trimethylsilylated by reaction with 200 μL of BSTFA + TMCS (*N*,*O*-bis (trimethylsilyl) trifluoroacetamide + trimethylchlorosilane, 99 : 1, Supelco) and 100 μL of pyridine (anhydrous, 99.8%, Sigma-Aldrich). The reaction mixture was heated at 70 °C for 1 h and analyzed on a Hewlett-Packard (HP) 5890 Series II gas chromatograph coupled to a HP 5971A mass selective detector with an Econo-Cap-EC-5 capillary column (30 m × 0.25 mm i.d., 0.25 μm film thickness) within 24 h. The 65 min temperature program of the GC initiated at 60 °C for 1 min, and then rose with a temperature ramp of 3 °C min^{-1} to 200 °C and isothermally held for 2 min, followed by another temperature ramp of 20 °C min^{-1} to 310 °C and isothermally held for 10 min. The temperatures of both the GC inlet and detector were at 250 °C.

2.3 Laboratory-generated SOA from β- and δ-IEPOX

SOA from acid-catalyzed reactive uptake of *trans*-β-IEPOX or δ-IEPOX was generated in the 10 m^3 indoor environmental smog chamber at the University of North Carolina as described previously.[9,23] Briefly, experiments were carried out under dark and wet conditions (50–55%, RH) at 295 ± 1 K. Prior to each experiment, the chamber was flushed continuously with clean air for ~24 hours corresponding to a minimum of seven chamber volumes until the particle mass concentration was <0.01 μg m^{-3} to ensure that there were no pre-existing aerosol particles. Chamber flushing also reduced VOC concentrations below the detection limit (~75 ppt for IEPOX) of an iodide-adduct high-resolution time-of-flight chemical ionization mass spectrometer (HR-TOF-CIMS). Operating details of the HR-TOF-CIMS have been previously described.[23] Temperature and RH in the chamber were continuously monitored using a dew point meter (Omega Engineering Inc.). Acidic $(NH_4)_2SO_4$ seed aerosol was injected into the pre-humidified chamber using a custom-built atomizer with an aqueous solution of 0.06 M $(NH_4)_2SO_4$ and 0.06 M H_2SO_4 until the desired total aerosol volume concentration (~75 $\mu m^3\ cm^{-3}$) was achieved. After seed injection, the chamber was left static for at least 30 min to ensure that the seed aerosol was stable and uniformly mixed. Then, 30 mg of *trans*-β- or δ-IEPOX was injected into the chamber at 2 L min^{-1} for 10 min and then 4 L min^{-1} for 50 min by passing high-purity nitrogen gas through a heated manifold (60 °C) containing an ethyl acetate solution of one of the IEPOX isomers described in Section 2.1.1.

On completion of IEPOX injection, a filter sample was collected for the subsequent offline analysis using HILIC (or RPLC)/ESI-HR-QTOFMS. Aerosols were collected onto a 47 mm Teflon filter (0.2 μm, Pall Scientific) in a stainless-steel filter holder for 30 min at a flow rate of 13.2 L min^{-1}. The filter sample along with a blank filter taken from the same batch on the day of the experiment were stored in a 20 mL scintillation vial at −20 °C prior to extraction and analysis. In addition to the filter sampling, SOA generated from the reactive uptake of IEPOX was collected using a particle-into-liquid sampler (PILS, Model 4001, Brechtel Manufacturing Inc. – BMI) system at the end of each experiment. The aerosols were sampled through an organic vapor denuder (Sunset Laboratory Inc.) and a 2.5 μm size-cut pre-impactor at a flow rate of ~12.5 L min^{-1}. The sample air flow was then mixed adiabatically with a steam flow heated at 98.5–100 °C in the PILS condensation chamber to produce high supersaturation of water vapor that grow particles to collectable sizes for collection onto a quartz impactor plate by inertial impaction. Impacted droplets were transferred by a wash-flow at ~0.55 mL min^{-1} through a debubbler and the resulting bubble-free sample liquid was delivered through a tubing with an inline filter into 2 mL poly vials held on an auto-collector (BMI) with a rotating carousel. Air sampling rate and wash-flow rate were examined and recorded before and after each experiment. Milli-Q water used in the wash-flow was spiked with 25 μM lithium bromide (LiBr, Sigma-Aldrich, 99.5%) as an internal standard to correct for dilution caused by condensation of water vapor during droplet collection. The dilution factor was typically from 1.1–1.2. The PILS vials were promptly stored under dark conditions at 2 °C upon collection until analysis. Chamber aerosol number distributions, which were subsequently converted to total aerosol surface area and volume concentrations, were monitored by a scanning electrical

mobility system (SEMS v5.0, BMI) containing a differential mobility analyzer (DMA, BMI) coupled to a mixing condensation particle counter (MCPC, Model 1710, BMI), in order to estimate the total aerosol mass. Summary of the experimental conditions can be found in Table S1.†

2.4 Field sample collection of $PM_{2.5}$

2.4.1 Look Rock, Tennessee, Southeastern U.S.. Quartz filter samples of $PM_{2.5}$ were collected at a field site (Look Rock, TN, USA) during the SOAS campaign in summer 2013 by a previously described procedure.[12] The filters were stored in the dark in a −20 °C walk-in freezer until chemical analysis. The sample selected for re-analysis was collected for three hours (16:00–19:00 local time) when one of the highest isoprene-derived SOA concentrations was measured during the campaign.[12,13]

2.4.2 Manaus, Brazil, Central Amazonia. $PM_{2.5}$ samples were collected from November 28–December 1 (transition of dry-to-wet season), 2016 on pre-baked Tissuquartz Filters (Whatman, 20 cm × 25 cm) using a high-volume $PM_{2.5}$ sampler (ENERGÉTICA with $PM_{2.5}$ Size Selective Inlet) located in the School of Technology of the Amazonas State University in Manaus, Brazil, near a major road. The high-volume $PM_{2.5}$ sampler was located 6 m above the ground and was equipped with a cyclone operated at 1.13 m^3 min^{-1}. Sampler was flow calibrated and the filter holder was cleaned with the filter extraction solvent (95 : 5 ACN/Milli-Q water for HILIC or methanol for RPLC) each day before sampling to ensure no carryover between samples. All filters were pre-baked for 12 h at 550 °C and all samples were collected for 24 h. $PM_{2.5}$ mass was determined by weighing filters before and after sampling (at 21 ± 2 °C, under <50% RH). Filters were stored at −18 °C in the dark until analysis. Similar to the sample selected from Look Rock, one sample (*i.e.*, November 30, 2016) selected for re-analysis had the highest loading of $PM_{2.5}$ and IEPOX-derived SOA tracers (*e.g.* 2-methyltetrols and C_5-alkene triols) measured by GC/EI-MS among all samples.

2.5 Sample preparation for offline analyses

2.5.1 2-Methyltetrol and methyltetrol sulfate standards. The 2-methyltetrol, 2-methyltetrol sulfate and 3-methyltetrol sulfate standards were stored at −20 °C until use. The standards were dissolved in a 2 mg mL^{-1} Milli-Q water solution, and then serially diluted immediately with 95 : 5 (v/v) ACN/Milli-Q water to 50, 10, 1, 0.25, 0.1, 0.025, and 0.01 μg mL^{-1} standards. The diluted standards were kept at 4 °C and analyzed within 24 h of preparation with the laboratory and field samples described below.

2.5.2 Laboratory-generated IEPOX SOA samples. Blank and sample filters of SOA generated from *trans*-β-IEPOX and δ-IEPOX were immersed in 22 mL of methanol and first extracted for 23 min by ultra-sonication, the water bath replaced with cool water, and then extracted again for 22 min. This was done to ensure the water bath inside the sonicator did not get too warm (from 25–30 °C, measured by a thermometer). The extracts were filtered through polypropylene membrane syringe filters and the solvent was evaporated under a gentle stream of nitrogen gas. Half of the dried methanol extracts were reconstituted with 150 μL of 95 : 5 (v/v) ACN/Milli-Q water and then diluted by a factor of 100 or 50, respectively for the β-IEPOX- and δ-IEPOX-derived SOA samples, in order to prepare the methyltetrol sulfates in the linear range of the calibration curves. The concentrations of the methyltetrol sulfates in the 150 μL reconstituted solutions were not saturated and calculated later to be 360–410 μg mL^{-1}, which were much lower than the solubility of the methyltetrol sulfates that were determined to be at least 2500 μg mL^{-1}; specifically, maximum solubility was determined by dissolving 25 mg of the methyltetrol sulfate standards in 10 mL of 95 : 5 (v/v) ACN/Milli-Q water. The aqueous PILS samples collected for the laboratory-generated IEPOX SOA near the end of the experiment were diluted by a factor of 20 using ACN in order to prepare them in 95 : 5 (v/v) ACN/Milli-Q water, and promptly analyzed using the HILIC/ESI-HR-QTOFMS method without any further pretreatment.

2.5.3 Field samples. A 37 mm-diameter punch from the quartz filter from Look Rock along with a lab blank filter were extracted as described above. Half of the Look Rock $PM_{2.5}$ extract was reconstituted with 150 μL of 95 : 5 (v/v) ACN/Milli-Q water and then diluted by a factor of 20.

Similarly, a 47 mm diameter punch from the selected quartz filter from Manaus, Brazil, as well as a lab blank filter, was extracted as described above. The residues were reconstituted in 1 mL methanol and a 0.3 mL aliquot was dried and reconstituted in 150 μL of 95 : 5 (v/v) ACN/Milli-Q water, and then diluted by a factor of 30 for analysis by HILIC/ESI-HR-QTOFMS.

3. Results and discussion

3.1 Separation of standards: 2-methyltetrols, 2- and 3-methyltetrol sulfates

The synthesized standards of 2-methyltetrols, 2- and 3-methyltetrol sulfates (Section 2.1.2) were analyzed by both RPLC and HILIC columns coupled to the ESI-HR-QTOFMS. As shown in the extracted ion chromatograms (EICs at m/z 215.023 ± 0.01) in Fig. 1, both 2- and 3-methyltetrol sulfate standards co-elute from the RPLC column as one peak at 1.5 min (Fig. 1(a1 and a2)). By contrast, the HILIC protocol resolved the 2-methyltetrol sulfate diastereomers at RTs of 4.2 and 5.2 min. (Fig. 1(b1) and S2†). The unambiguous synthetic route allows assignment of the diastereomers as the tertiary sulfates. Two additional trace peaks at RTs of 2.1 and 2.6 min are also resolved and assigned to the secondary methyltetrol sulfate diastereomers ((2*R*,3*S*)/(2*S*,3*R*)- and (2*S*,3*S*)/(2*R*,3*R*)-1,3,4-trihydroxy-3-methylbutan-2-yl sulfates) present as a trace impurity (<1%). The standard derived from hydrolysis of δ-IEPOX shows the predominant peaks at 8.0 and 8.3 min, assigned as the expected primary sulfate diastereomers (95.5%) (Fig. 2(a1) and S2†). A small quantity of the diastereomers at RTs of 2.1 and 2.6 min assigned to the secondary sulfates (~1.2%) is resolved, and the tertiary sulfates at 4.2 and 5.2 min are also present in a small amount (~6.7%) (Fig. 1(b2) and S2†). These results are in line with the resolution of diastereomers of methyltetrol sulfates observed in ambient aerosol by Hettiyadura *et al.* using similar HILIC

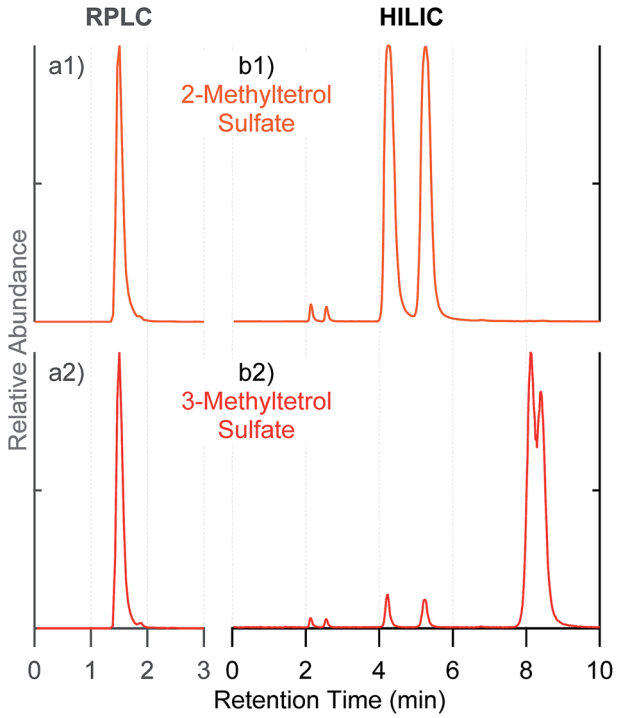

Fig. 1 Extracted ion chromatograms (EICs) at *m/z* 215.023 corresponding to methyltetrol sulfates. Using (a) RPLC C_{18} column, and (b) HILIC BEH amide column: standards of (1) 2-methyltetrol sulfates; (2) 3-methyltetrol sulfates. Standards were prepared at 10 μg mL^{-1}. No significant peaks were observed beyond the shown periods of retention time.

techniques; however, structural assignments in this past study were tentative and not based on unambiguous synthetic routes.[35,37] The secondary sulfate diastereomers in the HILIC trace of the standard derived by hydrolysis of δ-IEPOX are reasonably explained by a small yield of the less favored secondary hydrolysis product. The presence of 2-methyltetrol sulfates (tertiary sulfates) is surprising and will be discussed in more detail below in relation to the analysis of δ-IEPOX-derived SOA.

Comparison of the total ion chromatograms (TICs) acquired by RPLC and HILIC from an IEPOX-derived SOA in Fig. S3,† along with Fig. 1, unequivocally demonstrates the superiority of HILIC for resolving the multiple diastereomeric components of SOA, especially organosulfates derived from IEPOX.

Fig. 2(a1) shows that the deprotonated 2-methyltetrol diastereomers (racemic 2-methylerythritol and 2-methylthreitol) eluted at an identical RT of 4.0 min using the HILIC column. By contrast, GC/EI-MS analysis with prior derivatization is able to separate the 2-methyletrol diastereomers.[8,9,18] However, HILIC protocol is able to resolve diastereomers of 2- and 3-methyltetrol sulfates not resolvable by either GC/EI-MS or RPLC. Importantly, the 2-methyltetrols were simultaneously detected and resolved along with the methyltetrol sulfates. To our knowledge, this HILIC/ESI-HR-QTOFMS method presents the first time that the major IEPOX-derived SOA constituents, confirmed by authentic 2-methyletrols, 2- and 3-methyltetrol sulfates, have been chromatographically resolved and characterized by a single mass spectrometric technique operated with one column and ionization mode.

The linear dynamic range for the 2-methyltetrols was 0.01–25 μg mL^{-1} with a limit of detection (LOD) of 7.74 μg L^{-1} and a limit of quantification (LOQ) of 25.8 μg L^{-1} (Table 1). The linear dynamic range of 2-methyltetrol sulfates was 0.01–10 μg mL^{-1}, with an LOD of 1.72 μg L^{-1} and an LOQ of 5.75 μg L^{-1}. The linear dynamic range of 3-methyltetrol sulfates was 0.01–25 μg mL^{-1}, with an LOD of 3.83 μg L^{-1} and an LOQ of 12.8 μg L^{-1}. Coefficients of determination (R^2) values of the calibration curves ranged from 0.9994–1.0000. The linear dynamic ranges

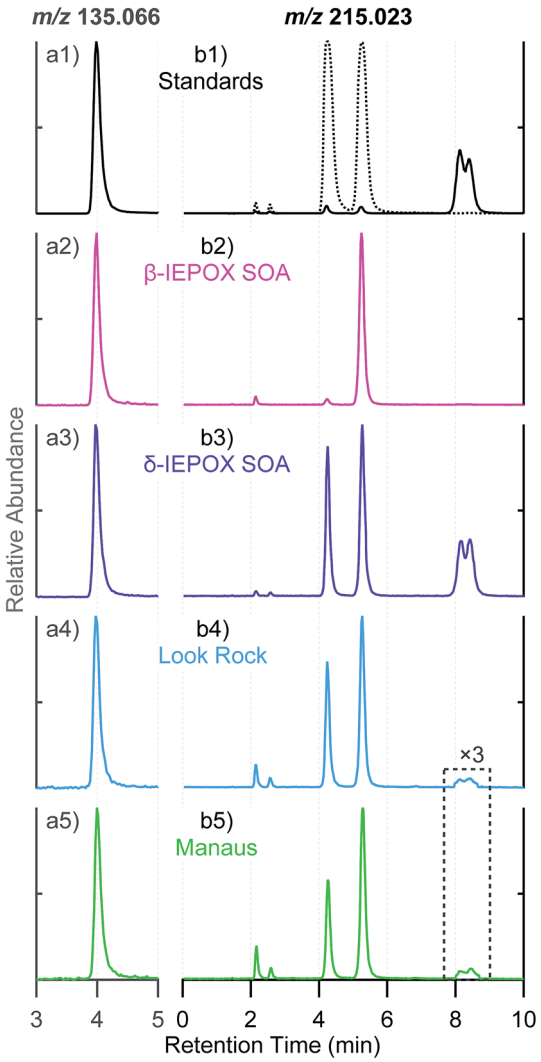

Fig. 2 EICs obtained from HILIC for (a) *m/z* 135.066 corresponding to 2-methyltetrols, (b) *m/z* 215.023 corresponding to methyltetrol sulfates from: (1) 10 μg mL^{-1} synthesized standard ((b1) 2-methyltetrol sulfates (dashed line) and 3-methyltetrol sulfates (solid line)); (2) laboratory-generated β-IEPOX SOA; (3) laboratory-generated δ-IEPOX SOA; (4) $PM_{2.5}$ sample collected at Look Rock during 2013 SOAS campaign; (5) $PM_{2.5}$ sample collected at Manaus in Nov. 2016. The laboratory-generated β-IEPOX SOA, δ-IEPOX SOA, Look Rock, and Manaus samples were diluted by a factor of 200, 100, 40, and 100, respectively. No significant peaks were observed beyond the shown periods of retention time.

of the organosulfates in this study are broader than those reported by Hettiyadura *et al.*, which ranged from 0.025–0.5 μg mL^{-1}.[35] The high R^2 and low LOQ values suggest the high performance of HILIC method is the most effective procedure for quantification of organosulfates in IEPOX-derived SOA.

3.2 Identification of 2-methyltetrols and methyltetrol sulfates in laboratory-generated SOA and ambient $PM_{2.5}$ samples

Authentic 2-methyltetrol, 2- and 3-methyltetrol sulfate standards were used to identify and quantify the corresponding SOA tracers. Fig. 2(a1–a5) compares the EICs at *m*/*z* 135.066, which correspond to the deprotonated 2-methyltetrols resolved on the HILIC column, from the 10 μg mL^{-1} standards of authentic 2-methyltetrols, aerosol filter extracts of laboratory-generated SOA derived from *trans*-β-IEPOX and δ-IPEOX, $PM_{2.5}$ samples from the Look Rock field site during 2013 SOAS campaign and from Manaus, Brazil in November 2016. The chromatographic peak at 4.0 min corresponding to the 2-methyltetrols were observed in all samples as the predominant peak, which demonstrates that HILIC/ESI-HR-QTOFMS can unequivocally identify the 2-methyltetrols in laboratory and ambient $PM_{2.5}$ samples.

Fig. 2(b1–b5) compares the EICs at *m*/*z* 215.023 of 10 μg mL^{-1} standards of authentic 2- and 3-methyltetrol sulfates, filter samples of laboratory-generated SOA derived from *trans*-β-IEPOX and δ-IEPOX, $PM_{2.5}$ samples collected from Look Rock during the 2013 SOAS campaign and from Manaus, Brazil in November 2016, respectively. The predominant primary sulfate diastereomers at RTs of 8.0 and 8.3 min in the 10 μg mL^{-1} 3-methyltetrol sulfate standard (Fig. 2(b1), solid line) are present as abundant components of the laboratory-generated δ-IEPOX SOA (Fig. 2(b3)) and as expected, were absent from the 10 μg mL^{-1} standard of the 2-methyltetrol sulfate (Fig. 2(b1), dashed line), and the laboratory-generated *trans*-β-IEPOX SOA (Fig. 2(b2)), confirming their origin as the acid-catalyzed multiphase chemistry of δ-IEPOX. In addition, the diastereomeric peaks at RTs of 4.2 and 5.2 min were unexpectedly present in Fig. 2(b3) as major SOA products from δ-IEPOX. This diastereomeric pair can be unequivocally assigned as the tertiary sulfates, which cannot be generated from δ-IEPOX without isomerization. Hence the trace in Fig. 2(b3) indicates importance of isomerization on reactive uptake of δ-IEPOX.[9] Furthermore, Fig. 2(b2) shows only a single significant product eluting at 5.2 min, indicating the presence of a single pair of enantiomer products. This peak is therefore indicative of *trans*-β-IEPOX as the source, but surprisingly requires that substitution at the tertiary carbon proceeds either with complete retention or complete inversion of optical configuration. Since the expected S_N1 substitution mechanism generally results in epimerization of asymmetric centers (*i.e.* diastereomeric products would be expected), the substitution is either extremely rapid or involves an S_N2 mechanism. Such observations will be helpful in studies to determine the origin and formation pathway of ambient methyltetrol sulfates. Full scan mass spectra of selected chromatographic peaks at *m*/*z* 215.023 in Fig. 2 are shown in Fig. S4.†

The 2- and 3-methyltetrol sulfates derived from β- and/or δ-IEPOX were present in ambient $PM_{2.5}$ SOA collected at the Look Rock and Manaus field sites (Fig. 2(b4 and b5)). The two diastereomers arising uniquely from δ-IEPOX (8.0, 8.3 min), and predominant in the 3-methyltetrol sulfate standard, were barely detected in the ambient aerosol samples. This observation supports (*cis*- or *trans*-) β-IEPOX as the predominant ambient IEPOX isomer, accounting for 97% of total ambient IEPOX,[16] which corroborates results based on ESI-ion mobility spectrometry (IMS)-HR-TOFMS as reported by Krechmer *et al.*[48] for the $PM_{2.5}$ collected from the Look Rock site during the 2013 SOAS campaign. Hence, the methyltetrol sulfate diastereomers at 2.1, 2.6, 4.2, 5.2 min support β-IEPOX isomers as the major contributor to the $PM_{2.5}$ collected at both of the Look Rock and Manaus field sites, which demonstrates the advantage of HILIC/ESI-HR-QTOFMS in differentiation of isomers and apportionment of reaction pathways.[9,12,18]

3.3 Quantification of 2-methyltetrols and methyltetrol sulfates in laboratory-generated SOA and ambient $PM_{2.5}$ samples

Concentrations of the 2-methyltetrols and methyltetrol sulfates in the laboratory-generated SOA collected by PILS and ambient $PM_{2.5}$ filters were quantified by HILIC/ESI-HR-QTOFMS and are summarized in Table 2. For the 2- and 3-methyltetrol sulfates, integrated areas of the 4–6 chromatographic peaks were

Table 2 Concentrations and mass fractions of 2-methyltetrols and methyltetrol sulfates measured from laboratory-generated SOA and ambient $PM_{2.5}$ samples by HILIC/ESI-HR-QTOFMS

	2-Methyltetrols		Methyltetrol sulfates	
	Mass conc.[a] (μg m^{-3})	% total mass[b]	Mass conc. (μg m^{-3})	% total mass
Laboratory β-IEPOX SOA	63.98	**33.9%**	109.67	**58.2%**
Laboratory δ-IEPOX SOA	29.49	**19.6%**	62.98	**41.9%**
Look Rock, TN, USA	0.861	5.6(7.5)%	2.334	15.3(12.9)%
Manaus, Brazil	0.137	(0.74)%	0.390	(1.34)%

[a] The mass concentrations of 2-methyltetrols and methyltetrol sulfates were measured from the PILS samples for the laboratory-generated SOA, and from the filter samples for the Look Rock and Manaus samples. [b] The total aerosol mass (organic + inorganic, shown in **bold**) was used for the mass closure for the laboratory-generated SOA, while the organic aerosol (or organic carbon, shown in parentheses) mass was used for the mass closure for the Look Rock and Manaus samples. The total aerosol mass was determined using an SEMS-MCPC system for the laboratory-generated SOAs, assuming the particle density to be 1.42 or 1.55 g cm^{-3} after reaction from β- or δ-IEPOX (ESI). The total organic aerosol mass for the Look Rock sample was measured by an ACSM.[11,12] The OC mass for the Look Rock and Manaus samples was measured using EC/OC analyzers. The relative analytical uncertainty in the quantification was determined to be up to ~14.1% (ESI).

summed to derive an overall response. As a result, the response factor (defined as the ratio of peak area to concentration) of the 2-methyltetrol sulfate standard was ~50% greater than that of the 3-methyltetrol sulfate standard. PILS sampling was chosen for better mass closures and to avoid uncertainties due to filter sampling artifacts and additional pretreatment procedures. Methyltetrol sulfates were quantified by an authentic 2-methyltetrol sulfate standard since the two major chromatographic peaks (RTs at 4.2 and 5.2 min) were consistently predominant in the standard and the $PM_{2.5}$ samples, except that authentic 3-methyltetrol sulfate was used as a standard to quantify methyltetrol sulfate in laboratory-generated SOA from δ-IEPOX. The percentage of 2-methyltetrols and methyltetrol sulfates in total aerosol mass is also shown in Table 2, calculated by dividing the mass concentration of each compound by the total aerosol mass obtained from SEMS-MCPC, assuming a particle density of 1.42 g cm^{-3} for β-IEPOX SOA or 1.55 g cm^{-3} for δ-IEPOX SOA (see ESI† for details). The analytical uncertainty in the quantification was determined to be up to ~14.1% (ESI†). As shown in Table 2, the concentration of the 2-methyltetrols in laboratory-generated *trans*-β-IEPOX-derived SOA was 63.98 μg m^{-3} (33.9% of total particle mass) and the concentration of methyltetrol sulfates was 109.67 μg m^{-3} (58.2% of total particle mass). In the laboratory-generated SOA from δ-IEPOX, the concentration of the 2-methyltetrols 29.49 μg m^{-3} (19.6% of total aerosol mass) and methyltetrol sulfates was 62.98 μg m^{-3} (41.9% of total aerosol mass). Together, the two IEPOX-derived SOA tracers contributed 92.1 ± 13.0% of the total aerosol mass from β-IEPOX and 61.5 ± 8.7% of the total aerosol mass from δ-IEPOX (Table 2). The methyltetrol sulfates account for approximately twice the 2-methyltetrol mass. The mass fractions of methyltetrol sulfates indicate conversion of a significant amount of inorganic sulfate seed aerosol to organosulfates, supported by measurements using ion chromatography for the PILS samples (Fig. S5†).

In addition to the monomeric methyltetrol sulfates (*m/z* 215.023), Fig. 3 shows that the HILIC column resolves multiple isomeric methyltetrol sulfate dimers (*m/z* 333.086) in laboratory SOA generated from β- and δ-IEPOX, suggesting oligomeric products as a likely source of the unaccounted for aerosol mass. RPLC did not resolve isomers of either species, since all water-soluble species co-eluted at ~2 min (Fig. S3†).[9,18] Additionally, small intensities of 2-methyltetrol dimers ($C_{10}H_{21}O_7^-$, *m/z* = 253.129) were detected in ambient samples from Look Rock and Manaus field sites. These dimers were not quantified due to the lack of authentic standards.

In the Look Rock $PM_{2.5}$ sample with the highest IEPOX-derived SOA concentration observed during the 2013 SOAS campaign,[12] the mass concentration of the 2-methyltetrol was measured by HILIC/ESI-HR-QTOFMS to be 0.86 μg m^{-3}, accounting for 5.6% of the total OA mass, or 7.5% of the total organic carbon (OC) mass. The total OA mass concentration averaged during the sampling period was determined to be 15.30 μg m^{-3} using an Aerodyne Aerosol Chemical Speciation Monitor (ACSM),[12] and the total OC mass concentration from the same sample was measured to be 5.04 μgC m^{-3} using a Sunset laboratory OC-elemental carbon (EC) aerosol analyzer.

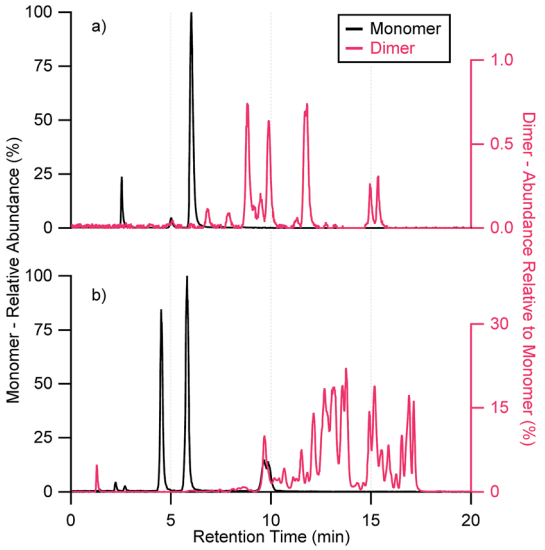

Fig. 3 EICs of *m/z* 215.023 ($C_5H_{11}O_7S^-$) and 333.086 ($C_{10}H_{21}O_{10}S^-$) corresponding to methyltetrol sulfate monomers and dimers, respectively, from (a) laboratory-generated β-IEPOX SOA diluted by a factor of 200; and (b) laboratory-generated δ-IEPOX SOA. No significant peaks were observed beyond 20 min.

Methyltetrol sulfates, quantified using the 2-methyltetrol sulfate standard, were determined to be 2.33 μg m^{-3}, accounting for 15.3% of the total OA (or 12.9% of the total OC) mass, and significantly higher than 1.14 μg m^{-3} measured by RPLC/ESI-HR-QTOFMS.[12] This discrepancy suggests that the RPLC/ESI-HR-QTOFMS method likely underestimates the methyltetrol sulfate concentrations, possibly resulting from insufficient dilution of Look Rock sample extracts (leading to concentrations beyond the linear range of the method), or appropriate isomeric standards, or caused by ion suppression due to co-elution with other water-soluble organic or inorganic aerosol components. The sum of the 2-methyltetrols and methyltetrol sulfates quantified by the new method accounted for 20.9 ± 2.9% of the total OA mass in the Look Rock sample during the 2013 SOAS campaign when high intensity of isoprene and anthropogenic emissions (acidic sulfate aerosol) were observed, making IEPOX-derived SOA the single largest contributor to the characterized OA constituents.[12]

For the Manaus sample, the HILIC/ESI-HR-QTOMS analysis measured 0.14 and 0.39 μg m^{-3} for 2-methyltetrols and methyltetrol sulfates, respectively, accounting for 0.74% and 1.34% of the total OC mass concentration (8.12 μgC m^{-3} for this particular sample collected on November 30, 2016) measured by a Sunset laboratory OC–EC aerosol analyzer. In addition, elevated concentrations of levoglucosan (0.46 μg m^{-3} by GC/EI-MS), EC (1.18 μgC m^{-3} by a Sunset OC-EC aerosol analyzer), and $PM_{2.5}$ (46.1 μg m^{-3}) were observed on this particular day, and more generally during the November 28–30, 2016, sampling period due to the large influence of biomass burning. In fact, average levoglucosan, OC, EC, and $PM_{2.5}$ concentrations during this biomass burning intensive period were 0.41 μg m^{-3}, 8.0 μgC m^{-3}, 1.3 μgC m^{-3}, and 43.6 μg m^{-3}, respectively. The elevated biomass burning likely explains why the IEPOX-derived

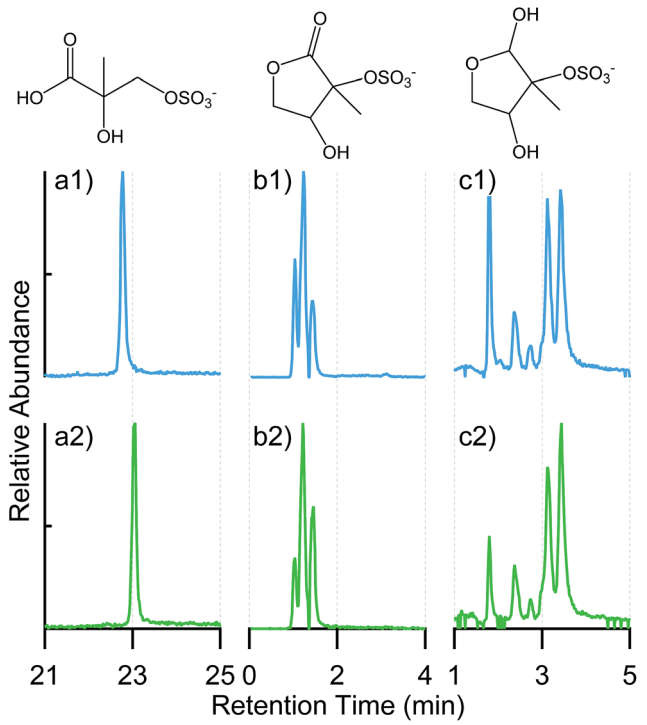

Fig. 4 EICs of other water-soluble organosulfates with their proposed structures: (a) m/z 199 corresponding to $C_4H_7O_7S^-$, (b) m/z 211 corresponding to $C_5H_7O_7S^-$, and (c) m/z 213 corresponding to $C_5H_9O_7S^-$ observed in $PM_{2.5}$ samples collected from (1) Look Rock during 2013 SOAS campaign; (2) Manaus in Nov. 2016. No significant peaks were observed beyond the shown periods of retention time.

SOA tracers accounted for a lower % contribution to the total OC mass *versus* the southeastern U.S. sample (Table 2), which the latter had little influences of biomass burning.

3.4 Other measurable water-soluble organic compounds in ambient $PM_{2.5}$

In addition to the targeted analysis for the 2-methyltetrols and methyltetrol sulfates, we were able to detect several other isoprene-derived organosulfates in the ambient $PM_{2.5}$ samples. Fig. 4 shows the EICs of organosulfates with chemical formulas $C_4H_7O_7S^-$ (m/z 199, accurate mass = 198.9912), $C_5H_9O_7S^-$ (m/z 213, accurate mass = 213.0069), and $C_5H_7O_7S^-$ (m/z 211, accurate mass = 210.9912) detected in the $PM_{2.5}$ samples from Look Rock and Manaus. These species have also been reported from other field and laboratory studies, including EICs obtained from HILIC/ESI-MS.[20,35–37] The ion of m/z 199 was confirmed as the sulfate ester derived from another isoprene SOA tracer 2-methylglyceric acid in high-NO_x conditions.[10,49] The structures of the m/z 211 and 213 were tentatively proposed with EICs consistent with previous observations.[20,36,37]

3.5 Discrepancy between HILIC/ESI-HR-QTOFMS and GC/EI-MS – thermal degradation of organosulfates

Table 3 lists the concentrations of 2-methyltetrols in samples of SOA from β-IEPOX, δ-IEPOX, Look Rock, and Manaus quantified in parallel by HILIC/ESI-HR-QTOFMS and GC/EI-MS with prior derivatization. The concentrations of 2-methyltetrols determined by GC/EI-MS were 204, 236, 160, and 288%, respectively, of that determined by HILIC/ESI-HR-QTOFMS. The discrepancies are consistent with suggestions that GC/EI-MS overestimates semi-volatile marker compounds because of thermal degradation of low volatile accretion products (*e.g.*, oligomers or possibly organosulfates).[28] To investigate whether the overestimation in fact resulted from thermal degradation or trimethylsilylation of the analytes, calibration curves of 2-methyltetrol, 2- and 3-methyltetrol sulfates were generated by GC/EI-MS along with the four SOA samples. As shown in Fig. 5/S6/S7(b and c), the isoprene-derived SOA tracers commonly observed by GC/EI-MS, including C_5-alkene triols, 2-methyltetrols, and 3-MeTHF-3,4-diols, were detected in the pure 2- and 3-methyltetrol sulfate standards. Fig. S6(b and c)† clearly illustrates the formation of 2-methyltetrols in the GC/EI-MS analysis of the 50 μg mL^{-1} 2- and 3-methyltetrol sulfate standards. The GC/EI-MS EIC of m/z 219 for the 50 μg mL^{-1} derivatized standard of authentic 2-methyltetrol diastereomer mixture is characterized by peaks at RTs of 34.0 and 34.8 min. Peaks with relative intensities of ~0.25 and ~5% at the same RTs characterize the EICs at m/z 219 of the pure 2- and 3-methyltetrol sulfate standards. The 2-methyltetrols from degradation of the organosulfates can partially explain the large discrepancy measured between the HILIC/ESI-HR-QTOFMS and GC/EI-MS methods. Other organosulfates and oligomers present in the aerosol samples may also contribute to the discrepancy. The C_5-alkene triol tracers for isoprene SOA, have been detected only by GC/EI-MS or SV-TAG methods.[8,9,17,30,50] Lopez-Hilfiker *et al.* have reported that the high concentrations of C_5-alkene triols measured in $PM_{2.5}$ samples analyzed by these procedures, in which samples are treated at high-temperature, are not consistent with their estimated volatility, and suggest that these compounds are degradation products of IEPOX-derived organosulfates and oligomers.[28] Based on the semi-quantitative relationship established for the C_5-alkene triols produced from the 2-methyltetrol sulfate standards prepared (ESI†), 30.0%, 42.8%, and 14.7% of the C_5-alkene triols measured by GC/EI-MS could be attributed to the potential thermal degradation of the 2-methyltetrol sulfates in the $PM_{2.5}$ samples from laboratory-generated β-IEPOX SOA, Look Rock, and Manaus, respectively (Table S2†). Similarly, 11.1% of the 2-methyltetrols and approximately all 3-MeTHF-3,4-diols in laboratory-generated δ-IEPOX SOA may be products of the thermal degradation of the 3-methyltetrol sulfates (Table S3†). As

Table 3 Concentrations and discrepancies of 2-methyltetrols (μg m^{-3}) from laboratory-generated SOA and ambient $PM_{2.5}$ samples measured by HILIC/ESI-QTOFMS and GC/EI-MS

2-Methyltetrols (μg m^{-3})	HILIC/ESI-QTOFMS	GC/MS	Ratio (GC/HILIC)
Laboratory β-IEPOX SOA	69.05	140.86	204%
Laboratory δ-IEPOX SOA	51.91	122.56	236%
Look Rock, TN, USA	0.861	1.381	160%
Manaus, Brazil	0.137	0.394	288%

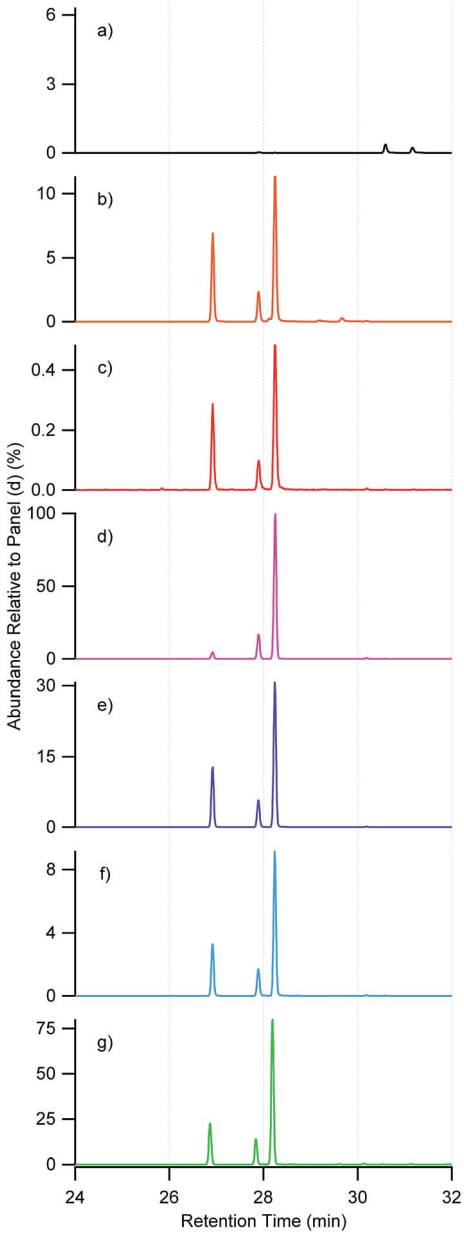

Fig. 5 GC/EI-MS EICs of *m/z* 231 corresponding to C_5-alkene triols (RT = 26.9, 27.9, 28.3 min) from: (a) 50 μg mL^{-1} standard of 2-methyltetrol; (b) 50 μg mL^{-1} standard of 2-methyltetrol sulfate; (c) 50 μg mL^{-1} standard of 3-methyltetrol sulfate; (d) laboratory-generated β-IEPOX SOA; (e) laboratory-generated δ-IEPOX SOA; (f) $PM_{2.5}$ sample at Look Rock during 2013 SOAS campaign; (g) $PM_{2.5}$ sample at Manaus in Nov. 2016. Note that the *y*-axis scale was adjusted to the highest peak in each panel, with the labelled abundance in percentage relative to that in panel (d).

demonstrated above, thermal degradation of organosulfates as well as low volatile accretion aerosol products (*i.e.*, oligomers) explains a substantial fraction of the isoprene-derived SOA tracers previously measured through analytical methods such as GC/EI-MS or SV-TAG in which samples are treated at high temperatures.[51] HILIC/ESI-HR-QTOFMS avoids such treatment and is therefore preferred for accurate quantification of IEPOX-derived SOA constituents.

4. Conclusion

The availability of authentic IEPOX-derived SOA standards was critical in developing the HILIC/ESI-HR-QTOFMS method described here. This protocol was used to evaluate IEPOX-derived SOA samples generated in laboratory studies or $PM_{2.5}$ samples collected from two isoprene-rich regions. The HILIC column can resolve the major water-soluble IEPOX-derived SOA constituents, including the 2-methyltetrols, methyltetrol sulfates and the corresponding dimers that are predicted to form in regional and global scale atmospheric chemistry models.[27,41–43,52–54] The major water-soluble IEPOX-derived SOA constituents can be quantified by one method with improved accuracy. We have demonstrated the ability to distinguish between different diastereomers of β- and δ-IEPOX-derived methyltetrol sulfates, which allows the contribution of the IEPOX isomers to be apportioned with the availability of authentic sulfate standards. Analysis by the HILIC method avoids high-temperatures required by GC/EI-MS or SV-TAG methods which cause degradation of IEPOX-derived organosulfates and oligomers to 2-methyltetrols, C_5-alkene triols, and 3-MeTHF-3,4-diols with consequent distortion of actual product distributions.[28,54]

By taking advantage of authentic standards and the HILIC/ESI-HR-QTOFMS method, we have estimated the mass fractions of the 2-methyltetrols and the methyltetrol sulfates in laboratory and ambient SOA samples. In summary, these two types of SOA constituents, likely the two largest contributors, contributed 92.1 ± 13.0%, 61.5 ± 8.7% to total aerosol mass, and 20.9 ± 2.9% to OA mass from the laboratory-generated β-IEPOX SOA, laboratory-generated δ-IEPOX SOA, and Look Rock $PM_{2.5}$, respectively. These two SOA constituents contributed ~2.1% to OC mass from Manaus $PM_{2.5}$ sample, which was likely lower owing to the fact that biomass burning was a large contributor to the OC mass during this sampling period whereas the Look Rock $PM_{2.5}$ sample had little influences of biomass burning. The methyltetrol sulfates are the largest single contributor to the IEPOX SOA mass, contributing ~2–3 times of the mass of the 2-methyltetrols. The predominant contributions of organosulfates (>90% of the reactive uptake of β-IEPOX) reveal the significance of conversion of inorganic sulfate to organosulfate, implying the critical role of inorganic sulfate as a nucleophile, and emphasize the importance of the multiphase chemistry of IEPOX leading to SOA formation in the isoprene-rich regions. In addition, oligomers derived from the methyltetrol sulfates and the 2-methyltetrols may explain the missing fraction of the total aerosol mass.

Large abundances of methyltetrol sulfates in atmospheric $PM_{2.5}$ could explain previous observations of the low-volatility nature of IEPOX-derived SOA in ambient aerosol.[28] The HILIC/ESI-HR-QTOFMS procedure described here can resolve water-soluble organic constituents from isoprene photochemical products generated *via* non-IEPOX pathways. HILIC separation can be interfaced to current RPLC/ESI-HR-QTOFMS procedures to develop two dimensional LC/ESI-HR-QTOFMS, further enhancing resolution of hydrophilic organic compounds in $PM_{2.5}$.

Conflicts of interest

The authors declare no conflict of interest.

Acknowledgements

This work was funded by the National Science Foundation (NSF) under Atmospheric and Geospace (AGS) Grant 1703535. This work was also support in part by the NSF under Chemistry (CHE) Grant 1404644, and CAPES Foundation by Brazil Ministry of Education, Brasilia, DF 70.040-020, Brazil. The UNC Biomarker Mass Spectrometry Facility, which contains the HILIC/ESI-HR-QTOFMS instrument, is supported by the National Institute for Environmental Health Sciences (NIEHS) Grant 5P20-ES10126.

References

1 Y. H. Wang, Z. R. Liu, J. K. Zhang, B. Hu, D. S. Ji, Y. C. Yu and Y. S. Wang, Aerosol physicochemical properties and implications for visibility during an intense haze episode during winter in Beijing, *Atmos. Chem. Phys.*, 2014, **15**(6), 3205–3215.

2 C. I. Davidson, R. F. Phalen and P. A. Solomon, Airborne particulate matter and human health: a review, *Aerosol Sci. Technol.*, 2005, **39**(8), 737–749.

3 M. C. Jacobson, H.-C. Hansson, K. J. Noone and R. J. Charlson, Organic atmospheric aerosols: review and state of the science, *Rev. Geophys.*, 2000, **38**(2), 267–294.

4 J. L. Jimenez, M. R. Canagaratna, N. M. Donahue, A. S. H. Prevot, Q. Zhang, J. H. Kroll, P. F. DeCarlo, J. D. Allan, H. Coe, N. L. Ng, A. C. Aiken, K. S. Docherty, I. M. Ulbrich, A. P. Grieshop, A. L. Robinson, J. Duplissy, J. D. Smith, K. R. Wilson, V. A. Lanz, C. Hueglin, Y. L. Sun, J. Tian, A. Laaksonen, T. Raatikainen, J. Rautiainen, P. Vaattovaara, M. Ehn, M. Kulmala, J. M. Tomlinson, D. R. Collins, M. J. Cubison, E. J. Dunlea, J. A. Huffman, T. B. Onasch, M. R. Alfarra, P. I. Williams, K. Bower, Y. Kondo, J. Schneider, F. Drewnick, S. Borrmann, S. Weimer, K. Demerjian, D. Salcedo, L. Cottrell, R. Griffin, A. Takami, T. Miyoshi, S. Hatakeyama, A. Shimono, J. Y. Sun, Y. M. Zhang, K. Dzepina, J. R. Kimmel, D. Sueper, J. T. Jayne, S. C. Herndon, A. M. Trimborn, L. R. Williams, E. C. Wood, A. M. Middlebrook, C. E. Kolb, U. Baltensperger and D. R. Worsnop, Evolution of organic aerosols in the atmosphere, *Science*, 2009, **326**(5959), 1525–1529.

5 K. S. Docherty, E. A. Stone, I. M. Ulbrich, P. F. DeCarlo, D. C. Snyder, J. J. Schauer, R. E. Peltier, R. J. Weber, S. M. Murphy, J. H. Seinfeld, B. D. Grover, D. J. Eatough and J. L. Jimenez, Apportionment of primary and secondary organic aerosols in Southern California during the 2005 study of organic aerosols in Riverside (SOAR-1), *Environ. Sci. Technol.*, 2008, **42**, 7655–7662.

6 A. Guenther, T. Karl, P. Harley, C. Wiedinmyer, P. I. Palmer and C. Geron, Estimates of global terrestrial isoprene emissions using MEGAN (Model of Emissions of Gases and Aerosols from Nature), *Atmos. Chem. Phys.*, 2006, **6**, 3181–3210.

7 W. L. Chameides, R. W. Lindsay, J. Richardson and C. S. Kiang, The role of biogenic hydrocarbons in urban photochemical smog: Atlanta as a case study, *Science*, 1988, **241**(4872), 1473–1475.

8 J. D. Surratt, S. M. Murphy, J. H. Kroll, N. L. Ng, L. Hildebrandt, A. Sorooshian, R. Szmigielsk, R. Vermeylen, W. Maenhaut, M. Claeys, R. C. Flagan and J. H. Seinfeld, Chemical composition of secondary organic aerosol formed from the photooxidation of isoprene, *J. Phys. Chem. A*, 2006, **110**(31), 9665–9690.

9 Y.-H. Lin, Z. Zhang, K. S. Docherty, H. Zhang, S. H. Budisulistiorini, C. L. Rubitschun, S. L. Shaw, E. M. Knipping, E. S. Edgerton, T. E. Kleindienst, A. Gold and J. D. Surratt, Isoprene epoxydiols as precursors to secondary organic aerosol formation: acid-catalyzed reactive uptake studies with authentic compounds, *Environ. Sci. Technol.*, 2012, **46**(1), 200–258.

10 Y.-H. Lin, H. Zhang, H. O. T. Pye, Z. Zhang, W. J. Marth, S. Park, M. Arashiro, T. Cui, S. H. Budisulistiorini, K. G. Sexton, W. Vizuete, Y. Xie, D. J. Luecken, I. R. Piletic, E. O. Edney, L. J. Bartolotti, A. Gold and J. D. Surratt, Epoxide as a precursor to secondary organic aerosol formation from isoprene photooxidation in the presence of nitrogen oxides, *Proc. Natl. Acad. Sci. U. S. A.*, 2013, **110**(17), 6718–6723.

11 S. H. Budisulistiorini, M. R. Canagaratna, P. L. Croteau, W. J. Marth, K. Baumann, E. S. Edgerton, S. L. Shaw, E. M. Knipping, D. R. Worsnop, J. T. Jayne, A. Gold and J. D. Surratt, Real-time continuous characterization of secondary organic aerosol derived from isoprene epoxydiols in downtown Atlanta, Georgia, using the Aerodyne aerosol chemical speciation monitor, *Environ. Sci. Technol.*, 2013, **47**(11), 5685–5694.

12 S. H. Budisulistiorini, X. Li, S. T. Bairai, J. Renfro, Y. Liu, Y. J. Liu, K. A. McKinney, S. T. Martin, V. F. McNeill, H. O. T. Pye, A. Nenes, M. E. Neff, E. A. Stone, S. Mueller, C. Knote, S. L. Shaw, Z. Zhang, A. Gold and J. D. Surratt, Examining the effects of anthropogenic emissions on isoprene-derived secondary organic aerosol formation during the 2013 Southern Oxidant and Aerosol Study (SOAS) at the Look Rock, Tennessee ground site, *Atmos. Chem. Phys.*, 2015, **15**, 8871–8888.

13 S. H. Budisulistiorini, K. Baumann, E. S. Edgerton, S. T. Bairai, S. Mueller, S. L. Shaw, E. M. Knipping, A. Gold and J. D. Surratt, Seasonal characterization of submicron aerosol chemical composition and organic aerosol sources in the southeastern United States: Atlanta, Georgia, and Look Rock, Tennessee, *Atmos. Chem. Phys.*, 2016, **16**, 5171–5189.

14 W. Rattanavaraha, K. Chu, S. H. Budisulistiorini, M. Riva, Y.-H. Lin, E. S. Edgerton, K. Baumann, S. L. Shaw, H. Guo, L. King, R. J. Weber, M. E. Neff, E. A. Stone, J. H. Offenberg, Z. Zhang, A. Gold and J. D. Surratt, Assessing the impact of anthropogenic pollution on isoprene-derived secondary organic aerosol formation in

PM2.5 collected from the Birmingham, Alabama, ground site during the 2013 Southern Oxidant and Aerosol Study, *Atmos. Chem. Phys.*, 2016, **16**, 4897–4914.

15 F. Paulot, J. D. Crounse, H. G. Kjaergaard, A. Kürten, J. M. S. Clair, J. H. Seinfeld and P. O. Wennberg, Unexpected Epoxide Formation in the Gas-Phase Photooxidation of Isoprene, *Science*, 2009, **325**(5941), 730–733.

16 K. H. Bates, J. D. Crounse, J. M. S. Clair, N. B. Bennett, T. B. Nguyen, J. H. Seinfeld, B. M. Stoltz and P. O. Wennberg, Gas Phase Production and Loss of Isoprene Epoxydiols, *J. Phys. Chem. A*, 2014, **118**(7), 1237–1246.

17 W. Wang, I. Kourtchev, B. Graham, J. Cafmeyer, W. Maenhaut and M. Claeys, Characterization of oxygenated derivatives of isoprene related to 2-methyltetrols in Amazonian aerosols using trimethylsilylation and gas chromatography/ion trap mass spectrometry, *Rapid Commun. Mass Spectrom.*, 2005, **19**, 1343–1351.

18 J. D. Surratt, A. W. H. Chan, N. C. Eddingsaas, M. Chan, C. L. Loza, A. J. Kwan, S. P. Hersey, R. C. Flagan, P. O. Wennberg and J. H. Seinfeld, Reactive intermediates revealed in secondary organic aerosol formation from isoprene, *Proc. Natl. Acad. Sci. U. S. A.*, 2010, **107**(15), 6640–6645.

19 J. D. Surratt, M. Lewandowski, J. H. Offenberg, M. Jaoui, T. E. Kleindienst, E. O. Edney and J. H. Seinfeld, Effect of acidity on secondary organic aerosol formation from isoprene, *Environ. Sci. Technol.*, 2007, **41**(15), 6640–6645.

20 J. D. Surratt, Y. Gomez-Gonzalez, A. W. H. Chan, R. Vermeylen, M. Shahgholi, T. E. Kleindienst, E. O. Edney, J. H. Offenberg, M. Lewandowski, M. Jaoui, W. Maenhaut, M. Claeys, R. C. Flagan and J. H. Seinfeld, Organosulfate formation in biogenic secondary organic aerosol, *J. Phys. Chem. A*, 2008, **112**, 8345–8378.

21 Y.-H. Lin, S. H. Budisulistiorini, K. Chu, R. A. Siejack, H. Zhang, M. Riva, Z. Zhang, A. Gold, K. E. Kautzman and J. D. Surratt, Light-absorbing oligomer formation in secondary organic aerosol from reactive uptake of isoprene epoxydiols, *Environ. Sci. Technol.*, 2014, **48**(20), 12012–12021.

22 C. J. Gaston, T. P. Riedel, Z. Zhang, A. Gold, J. D. Surratt and J. A. Thornton, Reactive uptake of an isoprene-derived epoxydiol to submicron aerosol particles, *Environ. Sci. Technol.*, 2014, **48**(19), 11178–11186.

23 T. P. Riedel, Y.-H. Lin, S. H. Budisulistiorini, C. J. Gaston, J. A. Thornton, Z. Zhang, W. Vizuete, A. Gold and J. D. Surratt, Heterogeneous reactions of isoprene-derived epoxides: Reaction probabilities and molar secondary organic aerosol yield estimates, *Environ. Sci. Technol. Lett.*, 2015, **2**(2), 38–42.

24 L. Xu, H. Guo, C. M. Boyd, M. Klein, A. Bougiatioti, K. M. Cerully, J. R. Hite, G. Isaacman-VanWertz, N. M. Kreisberg, C. Knote, K. Olson, A. Koss, A. H. Goldstein, S. V. Hering, J. de Gouw, K. Baumann, S. H. Lee, A. Nenes, R. J. Weber and N. L. Ng, Effects of anthropogenic emissions on aerosol formation from isoprene and monoterpenes in the southeastern United States, *Proc. Natl. Acad. Sci. U. S. A.*, 2015, **112**(1), 37–42.

25 M. Claeys, B. Graham, G. Vas, W. Wang, R. Vermeylen, V. Pashynska, J. Cafmeyer, P. Guyon, M. O. Andreae, P. Artaxo and W. Maenhaut, Formation of secondary organic aerosols through photooxidation of isoprene, *Science*, 2004, **303**(5661), 1173–1176.

26 T. P. Riedel, Y.-H. Lin, Z. Zhang, K. Chu, J. A. Thornton, W. Vizuete, A. Gold and J. D. Surratt, Constraining condensed-phase formation kinetics of secondary organic aerosol components from isoprene epoxydiols, *Atmos. Chem. Phys.*, 2016, **16**(3), 1245–1254.

27 S. H. Budisulistiorini, A. Nenes, A. G. Carlton, J. D. Surratt, V. F. McNeill and H. O. T. Pye, Simulating aqueous-phase isoprene-epoxydiol (IEPOX) secondary organic aerosol production during the 2013 Southern Oxidant and Aerosol Study (SOAS), *Environ. Sci. Technol.*, 2017, **51**(9), 5026–5034.

28 F. D. Lopez-Hilfiker, C. Mohr, E. L. D'Ambro, A. Lutz, T. P. Riedel, C. J. Gaston, S. Iyer, Z. Zhang, A. Gold, J. D. Surratt, B. H. Lee, T. Kurten, W. W. Hu, J. Jimenez, M. Hallquist and J. A. Thornton, Molecular composition and volatility of organic aerosol in the Southeastern U.S.: implications for IEPOX derived SOA, *Environ. Sci. Technol.*, 2016, **50**(5), 2200–2209.

29 G. Isaacman, N. M. Kreisberg, L. D. Yee, D. R. Worton, A. W. H. Chan, J. A. Moss, S. V. Hering and A. H. Goldstein, Online derivatization for hourly measurements of gas- and particle-phase semi-volatile oxygenated organic compounds by thermal desorption aerosol gas chromatography (SV-TAG), *Atmos. Meas. Tech.*, 2014, **7**(12), 4417–4429.

30 G. Isaacman-VanWertz, L. D. Yee, N. M. Kreisberg, R. Wernis, J. A. Moss, S. V. Hering, S. S. de Sá, S. T. Martin, M. L. Alexander, B. B. Palm, W. Hu, P. Campuzano-Jost, D. A. Day, J. L. Jimenez, M. Riva, J. D. Surratt, J. Viegas, A. Manzi, E. Edgerton, K. Baumann, R. Souza, P. Artaxo and A. H. Goldstein, Ambient gas-particle partitioning of tracers for biogenic oxidation, *Environ. Sci. Technol.*, 2016, **50**(18), 9952–9962.

31 B. J. Williams, Y. Zhang, X. Zuo, R. E. Martinez, M. J. Walker, N. M. Kreisberg, A. H. Goldstein, K. S. Docherty and J. L. Jimenez, Organic and inorganic decomposition products from the thermal desorption of atmospheric particles, *Atmos. Meas. Tech.*, 2016, **9**, 1569–1586.

32 H. Stark, R. L. N. Yatavelli, S. L. Thompson, H. Kang, J. E. Krechmer, J. R. Kimmel, B. B. Palm, W. Hu, P. L. Hayes, D. A. Day, P. Campuzano-Jost, M. R. Canagaratna, J. T. Jayne, D. R. Worsnop and J. L. Jimenez, Impact of thermal decomposition on thermal desorption instruments: advantage of thermogram analysis for quantifying volatility distributions of organic species, *Environ. Sci. Technol.*, 2016, **51**(15), 8491–8500.

33 Y. Gomez-Gonzalez, J. D. Surratt, F. Cuyckens, R. Szmigelski, R. Vermeylen, M. Jaoui, M. Lewandowski, J. H. Offenberg, T. E. Kleindienst, E. O. Edney, F. Blockhuys, C. Van Alsenoy, W. Maenhaut and M. Claeys, Characterization of organosulfates from the photooxidation of isoprene and

unsaturated fatty acids in ambient aerosol using liquid chromatography/(−) electrospray ionization mass spectrometry, *J. Mass Spectrom.*, 2008, **43**, 371–382.

34 A. J. Alpert, Hydrophilic-interaction chromatography for the separation of peptides, nucleic acids and other polar compounds, *J. Chromatogr. A*, 1990, **499**(19), 177–196.

35 A. P. S. Hettiyadura, E. A. Stone, S. Kundu, Z. Baker, E. Geddes, K. Richards and T. Humphry, Detection of atmospheric organosulfates using HILIC chromatography with MS detection, *Atmos. Meas. Tech.*, 2015, **8**, 2347–2358.

36 G. Spolnik, P. Wach, K. J. Rudzinski, K. Skotak, W. Danikiewicz and R. Szmigielski, Improved UHPLC-MS/MS methods for analysis of isoprene-derived organosulfates, *Anal. Chem.*, 2018, **90**(5), 3416–3423.

37 A. P. S. Hettiyadura, T. Jayarathne, K. Baumann, A. H. Goldstein, J. A. de Gouw, A. Koss, F. N. Keutsch, K. Skog and E. A. Stone, Qualitative and quantitative analysis of atmospheric organosulfates in Centreville, Alabama, *Atmos. Chem. Phys.*, 2017, **17**, 1343–1359.

38 P. Jandera, Stationary phases for hydrophilic interaction chromatography, their characterization and implementation into multidimensional chromatography concepts, *J. Sep. Sci.*, 2008, **31**(9), 1421–1437.

39 P. Hemstrom and K. Irgum, Hydrophilic interaction chromatograph, *J. Sep. Sci.*, 2006, **29**(12), 1784–1821.

40 Y. Guo and S. Gaiki, Retention behavior of small polar compounds on polar stationary phases in hydrophilic interaction chromatography, *J. Chromatogr. A*, 2005, **1074**(1–2), 71–80.

41 H. O. T. Pye, R. W. Pinder, I. R. Piletic, Y. Xie, S. L. Capps, Y. H. Lin and E. O. Edney, Epoxide pathways improve model predictions of isoprene markers and reveal key role of acidity in aerosol formation, *Environ. Sci. Technol.*, 2013, **47**(19), 11056–11064.

42 V. F. McNeill, Aqueous organic chemistry in the atmosphere: sources and chemical processing of organic aerosols, *Environ. Sci. Technol.*, 2015, **49**(3), 1237–1244.

43 E. A. Marais, D. J. Jacob, J. L. Jimenez, P. Campuzano-Jost, D. A. Day, W. Hu, J. Krechmer, L. Zhu, P. S. Kim, C. C. Miller, J. A. Fisher, K. Travis, K. Yu, T. F. Hanisco, G. M. Wolfe, H. L. Arkinson, H. O. T. Pye, K. D. Froyd, J. Liao and V. F. McNeill, Aqueous-phase mechanism for secondary organic aerosol formation from isoprene: application to the southeast United States and co-benefit of SO_2 emission controls, *Atmos. Chem. Phys.*, 2016, **16**(3), 1603–1618.

44 A. L. Bondy, R. L. Craig, Z. Zhang, A. Gold, J. D. Surratt and A. P. Ault, Isoprene-derived organosulfates: vibrational mode analysis by Raman spectroscopy, acidity-dependent spectral modes, and observation in individual atmospheric particles, *J. Phys. Chem. A*, 2018, **122**(1), 303–315.

45 Z. Zhang, Y.-H. Lin, J. D. Surratt, L. M. Ball and A. Gold, Technical Note: Synthesis of isoprene atmospheric oxidation products: isomeric epoxydiols and the rearrangement products *cis*- and *trans*-3-methyl-3,4-dihydroxytetrahydrofuran, *Atmos. Chem. Phys.*, 2012, **12**, 8529–8535.

46 A. Váradi, A. Gergely, S. Béni, P. Jankovics, B. Noszál and S. Hosztafi, Sulfate esters of morphine derivatives: Synthesis and characterization, *Eur. J. Pharm. Sci.*, 2011, **42**(1–2), 65–72.

47 H. Zhang, J. D. Surratt, Y.-H. Lin, J. Bapat and R. M. Kamens, Effect of relative humidity on SOA formation from isoprene/NO photooxidation: enhancement of 2-methylglyceric acid and its corresponding oligoesters under dry conditions, *Atmos. Chem. Phys.*, 2011, **11**, 6411–6424.

48 J. E. Krechmer, M. Groessl, X. Zhang, H. Junninen, P. Massoli, A. T. Lambe, J. R. Kimmel, M. J. Cubison, S. Graf, Y.-H. Lin, S. H. Budisulistiorini, H. Zhang, J. D. Surratt, R. Knochenmuss, J. T. Jayne, D. R. Worsnop, J. L. Jimenez and M. R. Canagaratna, Ion mobility spectrometry-mass spectrometry (IMS-MS) for on- and offline analysis of atmospheric gas and aerosol species, *Atmos. Meas. Tech.*, 2016, **9**, 3245–3262.

49 T. B. Nguyen, K. H. Bates, J. D. Crounse, R. H. Schwantes, X. Zhang, H. G. Kjaergaard, J. D. Surratt, P. Lin, A. Laskin and J. H. Seinfeld, Mechanism of the hydroxyl radical oxidation of methacryloyl peroxynitrate (MPAN) and its pathway toward secondary organic aerosol formation in the atmosphere, *Phys. Chem. Chem. Phys.*, 2015, **17**(27), 17914–17926.

50 S. S. de Sá, B. B. Palm, P. Campuzano-Jost, D. A. Day, M. K. Newburn, W. Hu, G. Isaacman-VanWertz, L. D. Yee, R. Thalman, J. Brito, S. Carbone, P. Artaxo, A. H. Goldstein, A. O. Manzi, R. A. F. Souza, F. Mei, J. E. Shilling, S. R. Springston, J. Wang, J. D. Surratt, M. L. Alexander, J. L. Jimenez and S. T. Martin, Influence of urban pollution on the production of organic particulate matter from isoprene epoxydiols in central Amazonia, *Atmos. Chem. Phys.*, 2017, **17**, 6611–6629.

51 A. Watanabe, S. J. Stropoli and M. J. Elrod, Assessing the Potential Mechanisms of Isomerization Reactions of Isoprene Epoxydiols on Secondary Organic Aerosol, *Environ. Sci. Technol.*, 2018, **52**(15), 8346–8354.

52 V. F. McNeill, J. L. Woo, D. D. Kim, A. N. Schwier, N. J. Wannell, A. J. Sumner and J. M. Barakat, Aqueous-phase secondary organic aerosol and organosulfate formation in atmospheric aerosols: a modeling study, *Environ. Sci. Technol.*, 2012, **46**(15), 8075–8081.

53 J. L. Woo and V. F. McNeill, SimpleGAMMA v1.0 – a reduced model of secondary organic aerosol formation in the aqueous aerosol phase (aaSOA), *Geosci. Model Dev.*, 2015, **8**, 1821–1829.

54 H. O. T. Pye, D. J. Luecken, L. Xu, C. M. Boyd, N. L. Ng, K. R. Baker, B. R. Ayres, J. O. Bash, K. Baumann, W. P. L. Carter, E. Edgerton, J. L. Fry, W. T. Hutzell, D. B. Schwede and P. B. Shepson, Modeling the current and future roles of particulate organic nitrates in the Southeastern United States, *Environ. Sci. Technol.*, 2015, **49**(24), 14195–14203.

